Optically Tagging Individual Particles in a Bed

ROBERT LEMLICH and MARK MANOFF

University of Cincinnati, Cincinnati, Ohio

Among certain operations involving large numbers of particles, such as fluidization or hindered settling, information regarding the movement of the particles can be of great value in understanding the operations themselves. For this reason the literature reports a number of theoretical and experimental investigations of this movement. In the latter category, optical methods applied to systems contained by glass or clear plastic have been used. However optical methods are by their nature limited to that which can be seen. This generally means limitation to the near vicinity of the bounding surfaces, since the particles naturally hide each other. To the present writers' knowledge, no optical scheme has been reported which allows the observer to peer from the outside into the interior of a swarm or bed of particles and freely follow the movement of one selected particle. Accordingly, a new experimental technique is suggested here for overcoming the problem of opacity for certain cases and allowing the observer to track a particle throughout its entire region of motion.

In essence, the principle is simple. It involves three steps.

1. Particles of a clear material are selected. As a trial, the authors selected 3-mm. glass spheres of the ordinary laboratory variety.

2. One particle is suitably marked for tracking by making it opaque. Depending on the objective of the prospective study, the particle selected for marking can be representative for a uniform bed, or it can be oversized, undersized, or differ from the average in some other way. By selectively marking only a portion of the particle, rotation as well as translation can be observed. If desired, several particles can be tracked simultaneously.

The marking process must be accomplished without changing any of the pertinent properties of the particle so that it will move among the other particles as though it were unmarked. For the present trial the bead was marked by exposing it to high intensity gamma radiation. This colored the bead dark brown but changed no other properties of consequence.

3. A working fluid is selected which is of the same optical index of refraction as the beads, or nearly so. This will make the bed of particles nearly transparent, with the opaque marked particle visible anywhere in their midst. The movement of the marked particle can then be followed visually, with motion pictures, or by stroboscopically illuminated still photography. Strategically mounted mirrors will allow simultaneous observation from two directions, thus locating the successive positions of the particle in three dimensions.

In the present trial, a liquid mixture consisting of 12% by volume of 1,1,2,2, tetrabromoethane in 1,1,2,2, tetrachloroethane was used. The indices of refraction of these two compounds straddle that of the glass beads, and the composition employed was obtained by titration to the closest approach to invisibility by daylight. Use of monochromatic light and beads of more uniform optical properties should make for more complete transparency.

The trial itself was simple. It involved observation of a 250-ml. beaker filled with glass beads, with a single opaque bead near the center of the bed. When the voids were filled with air or water, the marked bead was completely hidden from view.

However when the voids were filled with the aforementioned mixture of halogenated hydrocarbons, the marked bead was plainly visible from every direction. With the beads in motion, the movement of the marked bead could be easily followed.

Thus the method should offer a means for tracking and examining individual motion throughout a fluidized bed or other swarm of particles.

Ion Exchange Kinetics: A Comparison of Models

FREDERICK A. GLASKI and JOSHUA S. DRANOFF

Northwestern University, Evanston, Illinois

The kinetics of liquid-solid ion exchange reactions has been widely studied in recent years. This aspect of ion exchange has been considered from both theoretical and experimental points of view, and several different rate equations have been proposed. The objective of this note is to present the results of an analysis based on the most recent and rigorous model yet proposed for the ion exchange process. The model is developed and compared with two earlier models in the literature for one case of interest. The fit of all three models to experimental rate data is also considered.

The problem to be considered is the exchange which takes place when resin particles of one ionic form are contacted with a solution of different ions in a nonflow stirred reactor. The in-

Frederick A. Glaski is with Argonne National Laboratory, Lemont, Illinois, and J. S. Dranoff is with Columbia University, New York, New York.

stantaneous composition of both phases in this situation can be described by a suitable rate equation for the exchange process, combined with material balances and appropriate initial conditions.

For present purposes it will be assumed that at time zero V liters of solution containing cation species B^+ (with accompanying anion M^-) is contacted with w grams of resin particles containing only species A^+. The exchange which follows is indicated in Equation (1):

$$A_r^+ + B_s^+ \rightleftarrows A_s^+ + B_r^+ \qquad (1)$$

The subscripts r and s denote resin and solutions phases, respectively.

The equilibrium for such exchanges has been shown (*1*) to be represented by a selectivity constant K_{AB} defined as

$$K_{AB} = \frac{[A_s^+]\,[B_r^+]}{[A_r^+]\,[B_s^+]} \qquad (2)$$

where the bracketed quantities represent concentrations of the indicated species. These may conveniently be taken as milliequivalents per liter of solution for both phases.

The initial conditions corresponding to this type of experiment are

$$\text{at } t = 0,\ c_A = 0,\ c_B = c_M = C_0$$
$$q_A = Q_0,\ q_B = 0 \qquad (3)$$

Consideration of the equivalence of exchange reactions and of the overall material balance for species A^+ leads to the following relations, valid at any time t:

$$c_A + c_B = C_0 \qquad (4)$$

$$q_A + q_B = Q_0 \qquad (5)$$

$$c_A = Q_0 - q_A \qquad (6)$$

A differential material balance obtainable from Equation (6) introduces the rate expression

$$\frac{dc_A}{dt} = -\frac{dq_A}{dt} = R_A \qquad (7)$$

where R_A is the rate of exchange of A^+ in milliequivalents per liter per second.

The problem is completely described when an appropriate function is substituted for R_A. Three such functions arising from different models of the exchange process are considered here.

MASS ACTION MODEL

In this approach it is assumed that the exchange reaction rate may be written just as for a typical second-order reversible chemical reaction, that is

$$R_A = \frac{d\,[A_s^+]}{dt} = k_f\,[A_r^+][B_s^+] - k_b\,[A_s^+][B_r^+] \qquad (8)$$

(*Continued from page 425*)

INFORMATION RETRIEVAL

Small particle collection by supported liquid drops, Goldshmid, Yhuda, and Seymour Calvert, **A.I.Ch.E. Journal, 9,** No. 3, p. 352 (May, 1963).

Key Words: Collection Efficiency-8, Aerosols-8, Particles-8, Supported Drops-9, Inertia-7, Back collection-7, Interfacial Tension-6, Oscillation-6, Liquids-8, Drop Shattering-8.

Abstract: The collection of small particles (0.6 to 3.0μ) by single drops supported on hypodermic tubing was studied in a wind tunnel. Air velocities and ratios of particle to collector diameter were so chosen to exclude collection by diffusion and interception. The results are close to those expected for inertia collection down to 1μ particles, but were considerably higher for particles smaller than 1μ. A new mechanism of particle collection by the back of the drop was postulated and proved to explain this behavior. Interfacial tension between particle and drop was shown to have a predominant effect on the collection eff. The effect of drop oscillation on efficiency is negligible.

Total and form drag friction factors for the turbulent flow of air through packed and distended beds of spheres, Wentz, Charles A., Jr., and George Thodos, **A.I.Ch.E. Journal, 9,** No. 3, p. 358 (May, 1963).

Key Words: Pressure Drops-8, Friction Factors-7, Reynolds Number-6, Packed Beds-8, Distended Beds-8, Spheres-8.

Abstract: For the flow of air past packed and distended beds containing five layers of smooth plastic spheres, the total pressure drop has been measured across the middle layer of each bed for Reynolds numbers between 1,500 and 8,000. In addition, static pressure measurements were made around the surface of a test sphere located in the center of each bed, which could be independently rotated. The spheres were arranged in beds of cubic, body-centered cubic, and face-centered cubic configurations, having void fractions ranging from 0.354 to 0.882. These measurements permitted the calculation of friction factors which were related to the corresponding Reynolds numbers.

Rates of turbulent transfer to a pipe wall in the mass transfer entry region, Van Shaw, P., L. Philip Reiss, and Thomas J. Hanratty, **A.I.Ch.E. Journal, 9,** No. 3, p. 362 (May, 1963).

Key Words: Entry Region for Mass Transfer-8, Mass Transfer-8, Turbulent Transport-8, Pipe Turbulence-8, Concentration Polarized Electrodes-10, Concentration Sublayer-9, Length to Diameter Ratio-6, Wall Transport-8, High Schmidt Number-5, Stanton Number-7, Reynolds Number-6.

Abstract: Rates of transfer of mass from a fluid with a Schmidt number of 2,400 in fully developed turbulent flow to longitudinal sections of a pipe wall have been measured. The transfer section length was varied from 0.0177 to 4.31 pipe diameters, and the Reynolds number from 5,000 to 75,000. For L/d ratios from 0.0177 to 0.179, the Stanton number is proportional to $N_{Re}^{-.42}$ and to $(L/d)^{-1/3}$. For $L/d \geq 1.94$, at high Reynolds numbers, the measured Stanton numbers approach the fully developed values reported in the literature. The measurements described were made using a diffusion controlled electrode reaction.

Single particle studies of cation-exchange rates in packed beds: barium ion-sodium ion system, Kuo, James C. W., and M. M. David, **A.I.Ch.E. Journal, 9,** No. 3, p. 365 (May, 1963).

Key Words: A. Exchanging-8, Ion Exchange-8, Cation Exchange-8, Barium-9, Sodium-9, Beds-10, Packed-, Rates-8, Coefficients-8, Mass Transfer-8, Diffusivities-8, Internal-, Models-10, Mathematical-, Equilibria-8. **B.** Exchangers-9, Ion Exchangers-9, Cation Exchangers-9, Dowex 50W-X8-9, Particles-10, Beads-10, Single-, Homogeneity-8, Radioisotopes-10, Tracers-10.

Abstract: The rates of barium ion-sodium ion cation exchange in a packed bed were studied for both directions of exchange, with N/100 and 2N solutions, using single exchanger particles and radioactive tracer techniques. Exchange equilibria for the system were also measured. Liquid-film mass transfer coefficients for barium take-up agree with the j-factor correlation, but only overall coefficients could be obtained for the slower reverse reaction. Internal diffusion data are correlated quantitatively by a constant diffusivity model (with different diffusivities for the two directions) but qualitatively confirm a variable diffusivity model including electric field effects. The particles used showed excellent homogeneity of ion-exchange properties.

(*Continued on page 429*)

The foregoing equations may now be combined, with the introduction of equivalent fractions in the solution and resin phases, x and y respectively, in place of the concentrations listed above. The result is Equation (9), which, along with the revised initial condition, (10), completes the description of the problem:

$$\frac{dx_A}{dt} = k_b\ C_0\ (K_{AB} - 1)\ x_A^2 - k_b\ K_{AB}\ (Q_0 + C_0)x_A + Q_0\ k_b\ K_{AB} \tag{9}$$

$$x_A(0) = 0 \tag{10}$$

When all the constants are known, this equation may be readily integrated to give x_A as a function of time. The solution is, however, not of immediate interest here.

Rate equations of this type have been found to represent experimental data in a satisfactory manner (*2, 3, 4, 5, 6*) over small ranges of system variables, although the interpretation of such results has varied (*7, 8, 9, 10*). However, no serious theoretical justification for such a rate model has been made, and it has been largely discarded in favor of that to be described below (*6, 11*). On the other hand, it remains useful an an empirical form satisfactory for the usual ion exchange data.

ORDINARY FILM DIFFUSION MODEL

For this case, and that to follow, it is assumed that the rate of exchange depends solely on the rate of diffusion of the cations through a very thin film of relatively stagnant solution surrounding the resin particles. It is further assumed that the concentrations both in the external solution and throughout the resin are uniform. Thus, the only concentration gradients which exist are those across the film. Because the film is very thin, curvature may be neglected, thus permitting a linear analysis. In addition, the amount of either cation which accumulates within the film may be neglected in material balance considerations. Consequently, the diffusion process across the film may be considered to be at steady state, although the concentrations at both boundaries of the film are changing with time.

With these assumptions, the appropriate rate equation may be written. If Fick's law is now applied to the ionic diffusion, the flux across the film is as follows:

$$N_A = -D\frac{dc_A}{dz} \tag{11}$$

This approach should be strictly limited to isotopic exchange although it appears satisfactory in more general cases.

If Equation (11) is integrated over the film and equilibrium at the resin solution interface is assumed, the final differential equation for this case becomes

$$\frac{dx_A}{dt} = \frac{N_A S}{C_0 V} = \frac{D S}{\delta V}\left[\frac{K_{AB}\left(1 - \frac{C_0}{Q_0}x_A\right)}{1 + (K_{AB} - 1)\left(1 - \frac{C_0}{Q_0}x_A\right)} - x_A\right] \tag{12}$$

When combined with initial condition (10), this equation completes the description of the problem for the ordinary film diffusion case. Again, it should be noted that the equation may be integrated analytically if desired.

This type of model was originally considered by Boyd, Adamson, and Myers (*12*) and found to be successful in representing kinetic data when the solution concentration is low. It has also been used subsequently by others (*7, 6, 11*).

IONIC FILM DIFFUSION MODEL

A more recent and realistic approach to the film diffusion model has been suggested by Schlögl and Helfferich (*13*). They have recognized that ionic diffusion represents a coupled process in which virtual electrostatic potential gradients as well as concentration gradients play a part.

For the monovalent exchange being considered, the basic flux (Nernst-Planck) equations for the diffusion of species A^+, B^+, and M^- through the film are as follows (*14*):

$$\phi_A = -D_A\left[\frac{d\,c_A}{dz} + \frac{c_A F}{RT}\frac{d\psi}{dz}\right] \tag{13}$$

$$\phi_B = -D_B\left[\frac{d\,c_B}{dz} + \frac{c_B F}{RT}\frac{d\psi}{dz}\right] \tag{14}$$

$$\phi_M = -D_M\left[\frac{d\,c_M}{dz} - \frac{c_M F}{RT}\frac{d\psi}{dz}\right] \tag{15}$$

where ϕ and ψ represent ionic flux and electrostatic potential, respectively.

Since there is no net current flow or diffusion of anion in cation exchange processes

$$\phi_A + \phi_B + \phi_M = 0 \tag{16}$$

$$\phi_M = 0 \tag{17}$$

In addition, the principle of electroneutrality requires that at every point in the liquid phase

$$c_A + c_B = c_M \tag{18}$$

If Equations (15), (17), and (18) are combined, an expression for the potential gradient may be obtained:

$$\frac{F}{RT}\frac{d\psi}{dz} = \frac{1}{c_M}\frac{d\,c_M}{dz} = \frac{1}{c_A + c_B}\frac{d(c_A + c_B)}{dz} \tag{19}$$

This result may be then combined with (13), (14), and (16), to yield the basic flux equations:

$$\phi_A = -\frac{2\,D_A\,(c_A + c_B)}{\left(\frac{D_A}{D_B} + 1\right)c_A + 2\,c_B}\frac{d\,c_A}{dz} \tag{20}$$

$$\phi_B = -\frac{2\,D_B\,(c_A + c_B)}{\left(\frac{D_B}{D_A} + 1\right)c_B + 2\,c_A}\frac{d\,c_B}{dz} \tag{21}$$

At this point it can be seen that the introduction of the potential gradient term has resulted essentially in a standard flux equation but with a variable diffusivity, dependent on concentration. Since the ionic diffusivity is related to ionic mobility, see for example Denbigh (*15*), it can be shown that

$$\frac{D_A}{D_B} = r = \frac{u_A}{u_B} \tag{22}$$

In view of the availability of ionic mobility data the relation is most useful. The symbol r is used in the equations which follow.

It is now necessary to integrate either of these flux equations over the diffusion film. However, a relation between c_A and c_B must first be found for this region. If (20) and (21) are combined with (16), it will be seen that

$$\frac{d\,c_B}{d\,c_A} = -\frac{2\,D_A\,c_A + c_B\,(D_A + D_B)}{2\,D_B\,c_B + c_A\,(D_A + D_B)} \tag{23}$$

This may be integrated, assuming that when

$$c_A = x_A\ C_0$$
$$c_B = x_B\ C_0 = (1 - x_A)\ C_0 \tag{24}$$

to yield

$$c_B = -\left(\frac{r+1}{2}\right)c_A + \left[\left(\frac{r-1}{2}\right)^2 c_A^2 + c_0^2\,(1 - x_A + r\,x_A)\right]^{1/2} \tag{25}$$

Equation (25) thus relates c_A and c_B within the film in terms of the bulk solution composition x_A at the film-solution interface.

Finally, if Equation (25) is substituted into (20), the latter may be in-

tegrated across the film, exactly as with Equation (11), for model 2. The assumption of equilibrium at the film resin interface with this result leads to the following equation for the flux in terms of solution concentration:

$$\phi_A = \frac{D_A C_0}{\delta} [g(x_A)] \quad (26)$$

where:

$$g(x_A) = \left[\left\{ \frac{f_1(x_A)}{f_2(x_A)} \right\}^{1/2} - x_A + \left\{ \frac{f_1(x_A)}{f_2(x_A)} + \left(\frac{2}{r-1} \right)^2 f_1(x_A) \right\}^{1/2} - \left\{ x_A^2 + \left(\frac{2}{r-1} \right)^2 f_1(x_A) \right\}^{1/2} \right] \quad (27)$$

and

$$f_1(x_A) = 1 - x_A + r x_A \quad (28)$$

$$f_2(x_A) = \left(\frac{\rho x_A}{(1-\rho x_A) K_{AB}} \right)^2 + \left(\frac{\rho x_A}{(1-\rho x_A) K_{AB}} \right)(r+1) + r \quad (29)$$

This complex flux equation may be incorporated with the differential material balance to yield the final differential equation to be solved subject to initial condition (10).

$$\frac{dx_A}{dt} = \frac{D_A S}{\delta V} [g(x_A)] \quad (30)$$

In this case, the analytical integration of the equation is not readily apparent.

Thus far, three different models have been considered for the nonflow reactor problem. The equations which resulted—(9), (12), and (30)—differ considerably in form and might be expected, therefore, to yield distinctly different curves. This possibility was tested by comparison to some limited experimental data, to be shown below. It should be noted first, however, that each model contains essentially one usually unknown parameter. These are the rate constant k_b in Equation (9), the coefficient $\frac{DS}{\delta}$ in Equation (12), and the coefficient $\frac{D_A S}{\delta}$ in Equation (30). All of the other parameters would presumably be known from experimental conditions and literature data in each case.

EXPERIMENTAL TEST OF RATE MODELS

The data selected for comparison with the models discussed were taken from a recent study reported elsewhere by Glaski (*16*). Glaski studied the

(*Continued from page 427*)

INFORMATION RETRIEVAL

Mass transfer effects in surface catalysis, Ford, F. E., and D. D. Perlmutter, **A.I.Ch.E. Journal, 9,** No. 3, p. 371 (May, 1963).

Key Words: A. Reaction Data-1, Kinetic Data-1, Experimental Data-1, Mass Transfer Effects-8, Mass Transfer Rate-7, Quantitative Evaluation-2, Surface Catalysis-9, Computations-10, Agitation-6, Flow Rate-6, Correlations-5. B. Reactors-5, Comparison-10, Mass Transfer Effects-8, Literature-9.

Abstract: A criterion is developed which makes possible quantitative evaluation of mass transfer effects when they occur in conjunction with surface-catalyzed kinetics. The computations are based on experimental data for the particular reaction studied, and draw only in a summary way on the independent mass transfer correlations in the literature. Specific equations and inequalities are presented for three cases: first-order, second-order, and surface-concentration kinetics. Comparison with a series of literature reports shows the advantages of using the relations described here for interpreting existing measurements or planning an experimental program.

Natural convection evaporation from spherical particles in high-temperature surroundings, Pei, D. C. T., and W. H. Gauvin, **A.I.Ch.E. Journal, 9,** No. 3, p. 375 (May, 1963).

Key Words: Heat Transfer-8, Natural Convection-8, Mass Transfer-8, High Temperature-5, Spheres-5, Evaporation-8, Water-1, Methanol-1, Benzene-1, Temperature-6, Diameter-6, Heat Transfer-7, Evaporation-7, Mass Transfer-7, Chamber-10, Electrical Heat-10, Radiation-10.

Abstract: A two-dimensional analysis of the Prandtl boundary layer equations for natural convection, based on the finite radial velocity of the vapor evolved at the surface as the reference velocity is presented. To test this theoretical treatment, an experimental study of the rate of evaporation of water, methanol and benzene from stationary porous spheres was carried out in an electrically heated 9-in. diam. stainless steel spherical chamber. Three sizes of spheres were used: ¼, ⅜ and ½-in. in diam., and the temperature ranged from 400° to 1,000°K. The rates of heat transfer were satisfactorily correlated in terms of the dimensionless parameters predicted by the analysis.

The pumping capacity of impellers in stirred tanks, Marr, George R., Jr., and Ernest F. Johnson, **A.I.Ch.E. Journal, 9,** No. 3, p. 383 (May, 1963).

Key Words: Mixing-8, Stirred Tanks-8, Propellers-8, Pumping-8, Residence Time-8, Water-5, Baffles-5, Speed-6, Diameter-6, Correlation-9.

Abstract: A new experimental technique for determining the pumping capacity of impellers in stirred tanks is described. Data for marine propellers operated in a well-baffled tank are presented. It is shown that the pumping capacity of propellers is proportional to the product of propeller speed and the cube of propeller diameter.

Material and momentum transport in axisymmetric turbulent jets of water, Kiser, K. M., **A.I.Ch.E. Journal, 9,** No. 3, p. 386 (May, 1963).

Key Words: Jets-2, Fluid Flow-1, Conductivity Cell-10, Mixing Length-9, Eddy Diffusion-9, Mixing-8, Mass Transfer-8, Momentum Transfer-8, Turbulent Transport-8, Concentration-7, Water-5, Velocity-7.

Abstract: This paper presents some recent measurements on the rate of transport of sodium chloride in turbulent axisymmetric jets of water. Only mean values for velocity and concentration are considered and these are evaluated using classical transport theory.

As measured by the half-concentration radius, material is seen to spread linearly with distance downstream of the orifice beyond about ten orifice diameters. In this region for all practical purposes, both the velocity and the concentration profiles are affine. A value of 0.67 is obtained for the turbulent Schmidt number.

(*Continued on page 431*)

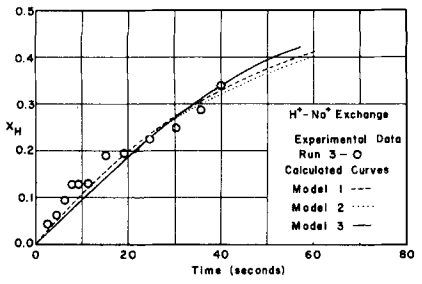

Fig. 1. Comparison of experimental and calculated data for the hydrogen ion-sodium ion exchange, run 3.

binary exchange of sodium ions and cesium ions with Dowex 50w-x8 resin in the hydrogen ion form. In reference to the previous equations, hydrogen ion may be regarded as ion A^+ and either sodium ion or cesium ion as ion B^+. The experiments were carried out at room temperature in aqueous chloride solutions, approximately 0.01N. At this concentration level external film diffusion should be the slow rate controlling process (*12*). Resin particles in the 40-50 mesh size range (wet hydrogen ion form) were used.

The reactor was made from a 4-liter glass beaker equipped with glass baffles and a glass mixer which provided vigorous agitation. The contents of the reactor were sampled by a specially constructed vacuum sampling apparatus which made it possible to withdraw in less than 1 sec. samples containing approximately 5 cc. of solution but no resin particles.

Experiments were made by rapid injection of a concentrated solution of the alkali chloride into the reactor, which contained up to 15 g of hydrogen ion form resin in 3 liters of distilled water. Successive timed samples were then taken and analyzed for the alkali ions. Complete compositions of both phases were later calculated for each sample using material balance considerations. The alkali solutions used contained measured fractions of the radioactive isotopes sodium-22 and cesium-137, and analysis of reactant solutions was made by scintillation counting in standard equipment.

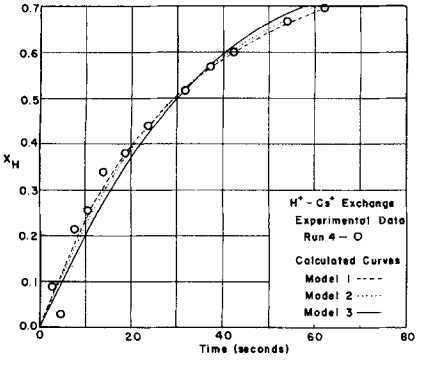

Fig. 2. Comparison of experimental and calculated data for the hydrogen ion-cesium ion exchange, run 4.

Two of Glaski's runs have been selected for present purposes. The conditions under which they were made are listed in Table 1. Also shown are measured equilibrium constants for these systems and calculated diffusivity ratios.

The actual rate data obtained from these runs are shown on Figures 1 and 2, where the fraction of hydrogen ions in solution phase is plotted against the time of reaction. Also shown on these figures are curves which correspond to the three models under consideration. These were calculated by integration, analytical or numerical as required, of the model equations. The curves shown represent the best fit to the data for each model, as determined by visual comparison. The corresponding values of the adjustable parameter for each model are listed in Table 2.

Examination of Figures 1 and 2 reveals that the experimental data for each run may be equally well represented by any of the three rate models discussed above. The calculated curves generally fit the data in a satisfactory manner and are not significantly different in appearance. Thus, although the rate equations have distinctly different forms, the integration of these equations serves to smooth out the differences in a striking way. This kind of behavior illustrates why it has been possible for various investigators to substantiate their claims for different rate equations. It points out once again the care necessary in the interpretation of kinetic data in general. The mere correspondence between limited experimental data and that calculated by a proposed model is not itself sufficient justification for the acceptance of the model. Rather, as has been shown in numerous chemical kinetics studies, any proposed model must be thoroughly examined and tested before it may be accepted as anything more than useful empiricism.

The present data obviously do not permit a distinction to be made among the models, although theoretical considerations lead one to the choice of the ionic diffusion model as the most appropriate for the situation at hand. However, it is felt that these results are significant for the following reasons:

1. The ionic diffusion model has been applied rigorously for the first time to the case of film controlled diffusion and has been shown to be compatible with experimental data. In view of this, such a model is certainly worthy of further investigation and consideration, despite the complexity of the formulation.

2. At the same time, it has been demonstrated once more that the simpler mass action and ordinary diffusion models retain an essential empirical utility. Although these formulations are clearly not acceptable from mechanistic or theoretical considerations, they are obviously satisfactory for the representation of data. Thus, these forms may continue to be of use for rapid everyday calculations within restricted ranges.

TABLE 1.

Run number	3	4
Exchange ions	H^+—Na^+	H^+—Cs^+
Solution concentration*, meq./ml.	0.0102	0.0096
Resin used†, meq.	30.45	57.54
Capacity ratio, ρ	1.0	0.5
Equilibrium constant, K	1.54	2.73
Diffusion ratio**, r	6.98	4.53

* Solution volume was 3.00 liters in all runs.
† Measured resin capacity was 4.74 meq./g. (dry H^+ form).
** Based on mobility data (*17*).

ACKNOWLEDGMENT

The experimental work reported here was made possible by a grant from the Research Corporation, and the numerical computations were carried out at the Northwestern University Computing Center under a grant from the National Science Foundation (G21511). This support is hereby acknowledged with thanks.

NOTATION

c = solution phase composition, meq./liter
C_0 = total solution cation concentration, meq./liter
D = effective diffusivity, liter/(cm.)(sec.)
F = Faraday's electrochemical equivalent constant
k = mass action rate constant, liters/(meq.)(sec.)
K_{AB} = mass action equilibrium constant
N = flux, excluding potential terms, meq./(sq.cm.)(sec.)
q = resin phase compositon, meq./liter
Q_0 = total resin cation capacity, meq./liter
r = diffusivity ratio, model 3

TABLE 2.

Run	3	4
Model 1: rate constant k_b, $\frac{\text{liters}}{(\text{meq.})(\text{sec.})}$	0.0008	0.00055
Model 2: coefficient $\frac{DS}{\delta}$, $\frac{\text{liters}}{\text{sec.}}$	0.012	0.026
Model 3: coefficient $\frac{D_A S}{\delta}$, $\frac{\text{liters}}{\text{sec.}}$	0.0174	0.032

R_A = rate of exchange, meq./(liter)(sec.)
R = gas law constant
S = total particle surface area, sq. cm.
t = time, seconds
T = temperature, °K.
u = ionic mobility, cm./sec.
v = total reactor solution volume, liters
x = equivalent fraction, solution phase
y = equivalent fraction, resin phase
z = distance measured in solution film around resin, cm.
δ = solution film thickness, cm.
ϕ = ionic flux in presence of electrostatic potential, meq./(sq. cm.)(sec.)
ψ = electrostatic potential, volts
ρ = ratio of total ionic equivalents present in solution phase to equivalents present in resin phase

Subscripts

A, B, M = refer to ionic species in question
b = reverse reaction
f = forward reaction
r = resin phase
s = solution phase

LITERATURE CITED

1. Kitchener, J. A., "Modern Aspects of Electrochemistry," No. 2, p. 115, Academic Press, New York (1959).
2. Thomas, H. C., *J. Am. Chem. Soc.*, **66**, 1664 (1944).
3. Nachod, F. C., and W. Wood, *ibid.*, 1380 (1944); *ibid.*, *67*, 629 (1945).
4. Juda, Walter, and Morris Carron, *ibid.*, **70**, 3295 (1948).
5. Dranoff, J. S., and Leon Lapidus, *Ind. Eng. Chem.*, **53**, 71 (1961).
6. Dickel, G., and A. Meyer, *Zeit. für Electrochemie*, **57**, 901 (1953).
7. Adamson, A. W., and J. J. Grossman, *J. Chem. Phys.*, **17**, 1002 (1949).
8. Gilliland, E. R., and R. F. Baddour, *Ind. Eng. Chem.*, **45**, 330 (1953).
9. Hiester, N. K., Theodore Vermeulen, et al., *A.I.Ch.E. Journal*, **2**, 404 (1956).
10. Sujata, A. D., J. T. Banchero, and R. R. White, *Ind. Eng. Chem.*, *47*, 2193 (1955).
11. Dickel, G., and L. V. Neciecki, *Zeit. Für Elektrochemie.*, **59**, 913 (1955).
12. Boyd, G. E., A. W. Adamson, and L. S. Myers, Jr., *ibid.*, **64**, 2836 (1947).
13. Schlogl, R., and Friedrich Helfferich, *J. Chem. Phys.*, **26**, 5 (1957).
14. Helfferich, Friedrich. "Ion Exchange," Chapter 6, McGraw-Hill, New York (1962).
15. Denbigh, K. G., "The Thermodynamics of the Steady State," p. 85, Methuen, London (1951).
16. Glaski, F. A., M.S. thesis, Northwestern University, Evanston, Illinois (1960).
17. Harned, H. S., and B. B. Owen, "The Physical Chemistry of Electrolytic Solutions," 3 ed., p. 233, Reinhold, New York (1958).

(Continued from page 429)

INFORMATION RETRIEVAL

The prediction of vapor-liquid equilibria using a theory of liquid mixtures, Sweeney, Robert F., and Arthur Rose, **A.I.Ch.E. Journal, 9,** No. 3, p. 390 (May, 1963).

Key Words: Equilibria (VLE)-8, Theory-8, Prediction-8, Experimental-8, Statistical Thermodynamics-10, Solutions Theory-10, Hexanol-Hexyl Acetate-9, Hexanol-Methyl Caproate-9, Hydrogen Bonding-9.

Abstract: Statistical thermodynamic calculations were applied to a quasi-lattice picture of liquid solutions in order to predict component activity coefficients and, subsequently, the vapor-liquid equilibria. The alcohol-ester binaries studied have two types of strong interactive forces between molecules. Behavior was adequately described by taking into account only the forces for these two types of interaction. Experimental data for the binaries n-hexanol-n-hexyl acetate and n-hexanol-methyl caproate were obtained during the course of this work.

Selectivity in experimental reactors, Tichacek, L. J., **A.I.Ch.E. Journal, 9,** No. 3, p. 394 (May, 1963).

Key Words: A. Kinetics-1, Axial Mixing-1, Diffusion Equations-10, Product Distribution-2. B. Kinetics-6, Axial Mixing-6, Homogeneous Reactions-8, Product Distribution-7. C. Reynolds Number-6, Schmidt Number-6, Peclet Number-6, Residence Time-6, Viscosity-6, Reactor Design-8, Reactor Flow-7, Reactor Length-7, Reactor Diameter-7. D. Peclet Number-6, Flow Reactors-8, Product Distribution-7. E. Experimental Reactors-10, Reactor Flow-6, Reactor Length-6, Reactor Diameter-6, Residence Time-6, Viscosity-6, Homogeneous Reactions-8, Product Distribution-7.

Abstract: An undesired distribution of products may result from homogeneous reactions within a flow reactor (unpacked tube) not designed and operated to minimize axial mixing. The effect of slight axial mixing on product distribution is examined theoretically for several types of kinetics. Distortion of product distribution, measured as loss in yield of the desired product (loss of selectivity) correlates with axial diffusivity. G. I. Taylor's theory of axial diffusion is subsequently used to relate reactor dimensions and flow to loss of selectivity; the effects are important in small-scale equipment. Design methods are given.

Rate factors in a heterogeneous catalytic system in a stirred reactor, Freeh, Edward J., Herbert G. Krane, and Aldrich Syverson, **A.I.Ch.E. Journal, 9,** No. 3, p. 400 (May, 1963).

Key Words: A. Model-1, Kinetics-8, Rate-8, Catalysis-8,9, Analysis-8, Mass Transfer-8, Resistance Concept-8, Chemical Reaction-9, Resistance Concept-10, Computer-10, Mathematical-, Heterogeneous-. B. Ethyl Oleate-1, Ethyl, Stearate-2, Nickel Catalyst-4, Hydrogenation-8, Catalysis-9, Reactor-10, Heterogeneous-. C. Ethyl Oleate-1, Ethyl Stearate-2, Correlation-8, Model-9, Rate-9, Chemical Reaction-9, Catalysis-9, Hydrogenation-9, Mathematical-, Heterogeneous-. D. Ethyl Oleate-1, Ethyl Stearate-2, Temperature-6, Pressure-6, Concentration-6, Rate-7, Mechanism-7,8, Chemical Reaction-9, Hydrogenation-9, Catalysis-9, Surface-9, Solution-9, Chemisorption-9, Desorption-9, Diffusion-9, Heterogeneous-. E. Ohio State University-, D-0262-.

Abstract: A computer-based method is presented for representing the rate behavior of systems involving both transport and kinetic processes, by use of mathematical models which employ a resistance concept to describe individual rate steps. Data obtained in the catalytic hydrogenation of ethyl oleate in a stirred reactor are used to illustrate the method. An analysis of the behavior of this system in terms of fractional resistances (allocation of total resistance among individual steps) shows that no one step is rate-controlling and that the relative importance of the several rate processes varies considerably with the reaction variables of temperature, pressure, and concentration.

Protruded sieve-tray performance, Teller, A. J., S. I. Cheng, and H. A. Davies, **A.I.Ch.E. Journal, 9,** No. 3, p. 407 (May, 1963).

Key Words: Liquid-Gas Contacting-10, Pressure Drop-7, Entrainment-7, Efficiency-7, Protrusion Geometry-6, Vapor Flow Rate-6, Distillation-8, Sieve Tray-10, Protruded Tray-10.

Abstract: Protrusion of perforations* in sieve-tray construction for liquid-gas contacting results in a decrease in dry pressure drop and entrainment dilution of liquid on a tray. For 3/16-in. diam. perforations with the protrusion geometry of 0.4-in. hip diam. and 0.1-in. protrusion above the tray, dry pressure drop over a wide range of vapor flow was reduced 50% and entrainment, from 50 to 80%, below that of a conventional sieve tray. Tray efficiency for the protruded tray remained essentially constant for $0.7<F<3.2$, in distillation tests.
* Patent pending.